



CHORUS

This is the accepted manuscript made available via CHORUS. The article has been published as:

Ability of $\text{TiO}_2(110)$ surface to be fully hydroxylated and fully reduced

Zhi-Tao Wang, Juan C. Garcia, N. Aaron Deskins, and Igor Lyubinetsky

Phys. Rev. B **92**, 081402 — Published 6 August 2015

DOI: [10.1103/PhysRevB.92.081402](https://doi.org/10.1103/PhysRevB.92.081402)

On Ability of TiO₂(110) Surface to Be Fully Hydroxylated and Fully Reduced

Zhi-Tao Wang,¹ Juan C. Garcia,² N. Aaron Deskins,² and Igor Lyubinetsky^{1,*}

¹*EMSL, Institute for Integrated Catalysis, and Pacific Northwest National Laboratory, Richland, WA 99352,*

²*Department of Chemical Engineering, Worcester Polytechnic Institute, Worcester, MA 01609*

Many TiO₂ applications (e.g., in heterogeneous catalysis) involve contact with ambient atmosphere and/or water. The resulting hydroxylation can significantly alter its surface properties. While behavior of single, isolated OH species on the model metal oxide surface of rutile TiO₂(110) is relatively well understood, much less is known regarding highly-hydroxylated surfaces and/or whether TiO₂(110) could be fully hydroxylated under ultra-high vacuum conditions. Here we report in-situ formation of a well-ordered, fully-hydroxylated TiO₂(110)-(1 × 1) surface using an enhanced photochemical approach, key parts of which are pre-dosing of water and multi-step dissociative adsorption and subsequent photolysis of the carboxylic (trimethyl acetic) acid. Combining scanning tunneling microscopy, ultra-violet photoelectron spectroscopy and density functional theory results, we show that the attained “super OH” surface is also fully reduced, as a result of the photochemical trapping of electrons at the OH groups.

PACS numbers: 68.37.Ef, 68.47.Gh, 82.37.Vb, 73.43.Cd

* Corresponding author: igor.lyubinetsky@pnnl.gov

TiO₂-based materials play a central role in catalysis, solar energy generation, and health and environmental sciences. Since many applications take place under ambient conditions and/or water, hydroxyl groups are virtually omnipresent at TiO₂ surfaces. Both chemical and physical properties of TiO₂ surfaces can be significantly affected by the presence of hydrogen [1, 2]. It is also presumed that surface hydroxyls are important players in many catalytic processes [3-7]. Furthermore, the hydrophilicity of TiO₂ surface may correlate with an increase of OH concentration [8], whereas OH species are suggested to act as nucleation sites for water adsorption [9]. The majority of fundamental research of hydrogen on TiO₂ has been carried out on the model rutile (110)-(1 × 1) surface [1, 10, 11]. However, while behavior of single, isolated OH species on TiO₂(110) has been intensively studied and relatively well understood [1, 10], there were just a few attempts to prepare and examine surfaces hydroxylated close to saturation [12-14].

Standard TiO₂(110) preparation by ion sputtering and annealing in ultra-high vacuum (UHV) leads to the creation of intrinsic point defects such as subsurface Ti interstitials and surface oxygen vacancies (V_O 's) [1, 15]. Hence, the most common way for preparation of the hydroxylated TiO₂(110) surface is via water dissociation at the V_O 's, replacing each vacancy with two hydroxyl species [2]. However, this results only in a partial hydroxylation, with a maximum OH coverage, $\Theta(\text{OH})$, twice that of V_O 's. Typically, V_O concentration does not exceed ~ 0.15 ML for the (1 × 1) surface [1]. Furthermore, the ambient pressure x-ray photoelectron spectroscopy has shown that $\Theta(\text{OH})$ is still limited (by V_O concentration) even at relative humidities of 100% [9]. On the other hand, a higher degree of TiO₂(110) hydroxylation can be achieved with several other techniques that do not depend on the presence of V_O 's [12, 13]. In particular, the surface can be hydroxylated via electron irradiation of thin water films absorbed at low temperatures and followed by thermal desorption [12], or by exposure to atomic hydrogen [13]. Note that while the hydroxylation of V_O 's by H₂O dissociation does not affect the reduction state of the surface [16, 17], an exposure to atomic H does lead to additional reduction [18]. Nevertheless, it appears that the TiO₂(110) cannot be fully hydroxylated by any of these methods, with a highest $\Theta(\text{OH}) < 0.7$ ML reported [14]. Consequently, intriguing questions arise whether the TiO₂(110) surface could be fully hydroxylated ($\Theta(\text{OH}) = 1$ ML) at all and/or what redox state of such surface would be.

We have recently introduced the novel photochemical route for preparation of highly-hydroxylated (up to 0.5 ML OH coverage) $\text{TiO}_2(110)$ surface, which is based on deprotonation and subsequent photolysis of the trimethyl acetic acid (TMAA) [19]. Lately, this technique has been adopted by using photo-splitting of methanol for $\text{TiO}_2(110)$ hydroxylation [20]. However, the attained $\text{TiO}_2(110)$ surfaces were not entirely organics-free, and their redox states were uncertain [20, 21]. In this Letter, using enhanced technique that employs pre-adsorption of water and a multi-step approach for sequential dissociative adsorption/photolysis of TMAA, we report the first preparation of a well-ordered, fully-hydroxylated and organics-free $\text{TiO}_2(110)$ - (1×1) surface, as evidenced by scanning tunneling microscopy (STM). Furthermore, the ultra-violet photoelectron spectroscopy (UPS) and density functional theory (DFT) results demonstrate that the attained “super OH” surface is fully-reduced.

Figure 1 illustrates our strategy for the formation of fully-hydroxylated $\text{TiO}_2(110)$ surface. The top left panel in Fig. 1 displays the structure of a starting surface of clean reduced $\text{TiO}_2(110)$, consisting of alternating rows of 5-fold coordinated Ti atoms (Ti_{5c}) and 2-fold coordinated bridging O atoms (O_b), and having a limited number of bridging V_O defects. The process is initiated with adsorption of water in Step I (which as all other steps is carried out at 300 K) [22]. As discussed earlier, H_2O dissociation at the V_O sites results in a partial hydroxylation of the surface via formation of bridging hydroxyl (OH_b) pairs, reaching maximum OH_b coverage that is twice that of V_O 's [1, 10]. More importantly though, this step also removes the V_O sites, a characteristic that would be advantageous in the next step. In turn, Step II consists of two segments: 1) the saturation exposure of the partially hydroxylated $\text{TiO}_2(110)$ with TMAA molecules ($(\text{CH}_3)_3\text{CCOOH}$) and 2) the irradiation with ultra-violet (UV) light. It is known that TMAA species adsorb dissociatively through deprotonation, whereas the carboxylate group of the trimethyl acetate ($(\text{CH}_3)_3\text{CCOO}$, TMA) bridge-bonds across two Ti_{5c} 's and the acid proton forms an adjacent OH_b group [23, 24]. Therefore, for the saturation TMA coverage of 0.5 ML, an additional 0.5 ML of OH_b 's is generated concurrently. The subsequent UV irradiation selectively removes all TMA species while leaving OH_b species intact [19, 23]. As a result, Step II produces a highly-hydroxylated surface with accumulated $\Theta(\text{OH}_b)$ above 0.5 ML, which is also TMA-free. Later is ensured by Step I, which via the hydroxylation of V_O sites prevents TMAA adsorption there that, otherwise, would result in the formation of photobind TMA species at V_O 's [21]. Finally, Step III basically repeats Step II one more time. It adds still more

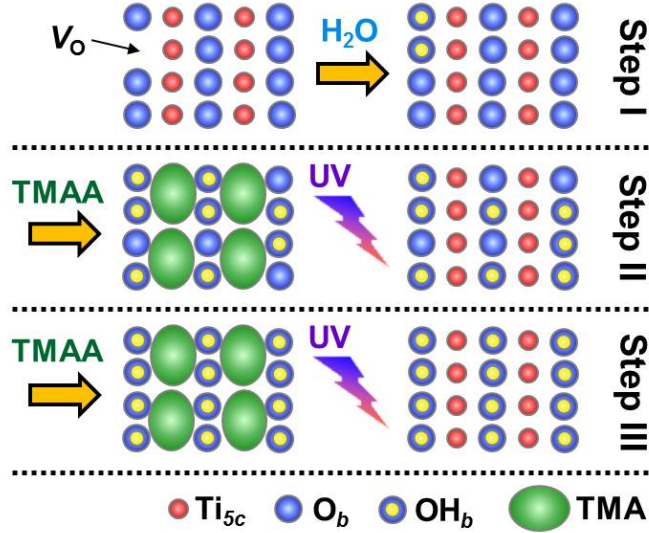


Figure 1. Three-step approach for preparation of fully-hydroxylated TiO₂(110) surface. Step I involves dissociative adsorption of H₂O at the V_O sites, while both Step II and Step III involve the saturation exposure with TMAA molecules followed by irradiation with UV light. (TMAA is added to the final stage of Step I (II) to produce the first stage of Step II (III)).

OH_b species, providing the remaining OH_b's for a saturation coverage of 1 ML, and, thus, potentially attaining a fully-hydroxylated TiO₂(110) surface.

We have acquired STM images after completing each individual step of the proposed method, as shown in Figure 2. In a typical STM image of the initial clean reduced TiO₂(110) surface in Fig. 2(a), approximately 0.07 ML of V_O 's are seen as a faint bright spots on the dark O_b rows. After quasi-saturation exposure to H₂O in Step I, the H₂O dissociation at the V_O sites results in the appearance of a number of OH_b species, observed as slightly brighter spots in Fig. 2(b), also centered on O_b rows. On the other hand, almost no V_O sites are seen, which reflects a nearly complete hydroxylation of the V_O 's and is consistent with the detected $\Theta(\text{OH}_b)$ of ~ 0.13 ML. In the first segment of Step II, the partially-hydroxylated (and V_O -free) surface was dosed with TMAA up to saturation, resulting in the formation of a dense TMA monolayer ($\Theta(\text{TMA}) \sim 0.49$ ML), as seen in Fig. 2(c). The individual TMA species are seen as ordered round bright spots centered at Ti_{5c} rows, forming the (2×1)-reconstructed domains (consistent with TMA occupation of two adjacent Ti_{5c} sites) [23, 24.]. Although the same coverage (~ 0.49 ML) of OH_b's is added upon TMAA deprotonation, OH_b groups are virtually invisible to STM

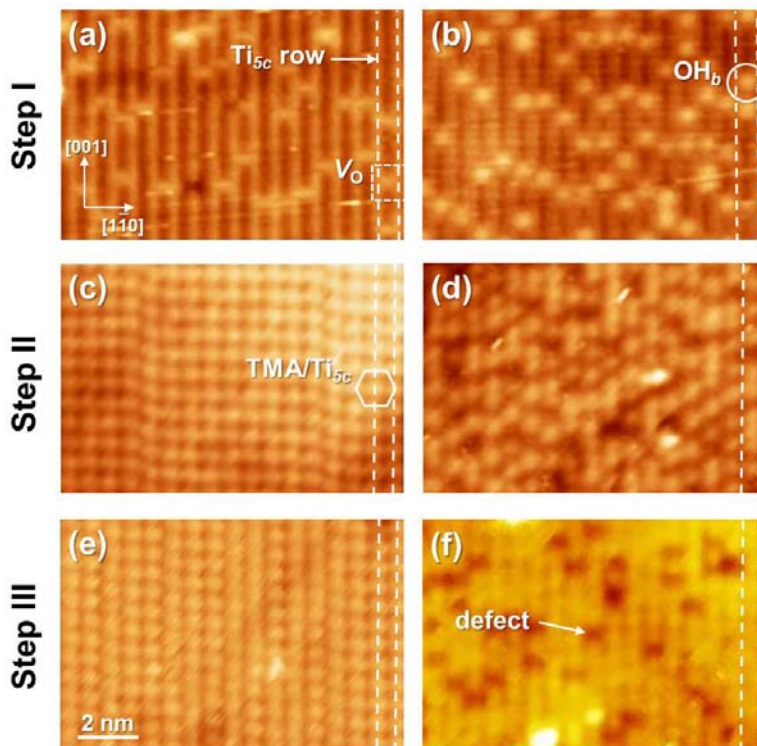


Figure 2. STM images of $\text{TiO}_2(110)$ after each consecutive segment in the proposed three-step formation process of the fully-hydroxylated surface: (a) clean reduced surface ($\Theta(V_O) \sim 0.07$ ML), and after (b) saturation H_2O exposure ($\Theta(\text{OH}_b) \sim 0.13$ ML), (c) first TMAA saturation ($\Theta(\text{TMA}) \sim 0.49$ ML), (d) first UV irradiation ($\Theta(\text{OH}_b) \sim 0.61$ ML), (e) second TMAA saturation ($\Theta(\text{TMA}) \sim 0.49$ ML), and (f) second UV irradiation ($\Theta(\text{OH}_b) \sim 0.92$ ML). All steps were carried out at 300 K. (Imaging parameters: $V_{\text{sample}} = +1.5$ V, $I_{\text{tunnel}} = 30$ pA).

observation while residing beside much larger TMA species [24, 25]. After prolonged UV irradiation in the second segment of Step II, practically all TMA's are photodepleted, making the non-photoreactive OH_b species visible in Fig. 2(d) [19, 21]. While the surface is somewhat less ordered on a long-range scale, locally, the onset of the across-row alignment of the OH_b "chains" into (2×1) - and/or (1×1) -ordered patterns can be seen. (The observed darker spots correspond to non-hydroxylated O_b sites). The determined $\Theta(\text{OH}_b) \sim 0.61$ ML is rather close to the accumulated coverage anticipated after the first two steps (0.62 ML). Afterward, the resulting surface was once more dosed with TMAA in the first segment of Step III. Figure 2(e) shows that again the close-packed (2×1) -ordered TMA monolayer is formed, which looks nearly identical to the one produced in Step II, and demonstrates that highly-hydroxylated surface does not inhibit

further TMAA adsorption. (Since there is not enough O_b sites to accommodate additional 0.5 ML of H atoms, some of them could be consumed in the formation and spontaneous desorption of H_2O molecules upon TMAA adsorption at the highly-hydroxylated surface). Following UV irradiation in the last segment of the process, Fig. 2(f) reveals the TMA-free, yet still further hydroxylated surface ($\Theta(OH_b) \sim 0.92$ ML). The obtained surface exhibits an ordered (1×1) -structure, which is also reflected in a sharp (1×1) low energy electron diffraction pattern shown in Fig. S1 in the Supplemental Material [22]. A small amount (~ 0.08 ML) of distinct, mostly isolated dark spots centered on the O_b rows seen in Figure 1f, apparently are defects, likely corresponding to single H “vacancies” (non-hydroxylated O_b sites). Nevertheless, the attained surface, with OH_b coverage just slightly below 1 ML, clearly demonstrates that a $TiO_2(110)$ surface can be effectively *fully-hydroxylated*.

In an attempt to come even closer to an OH_b coverage of 1 ML, we have applied to the obtained surface (with $\Theta(OH_b) \sim 0.92$ ML) an additional step of TMAA dosing/UV irradiation. STM images in Fig. S2 once again indicate the formation of a typical saturated TMA monolayer and its subsequent photodepletion. However, the extent of hydroxylation practically did not change as the resulting surface has a comparable $\Theta(OH_b) \sim 0.93$ ML. This surface has somewhat less amount of H vacancies (~ 0.02 ML), but a number of additional bright spots (~ 0.05 ML) located on the O_b rows are also observed. They are attributed to the non-photoreactive TMA species, residing at newly created V_O sites [21]. In turn, these new V_O 's are likely generated upon spontaneous desorption of H_2O (via a recombination of the acid proton with an existing adjacent OH_b group upon TMAA deprotonation), as mentioned above. It is conceivable that the probability of such a reaction would be non-negligible only at close to saturation OH_b coverages. Hence, we speculate that this process is likely responsible for a limiting maximum OH_b coverage of the hydroxylated $TiO_2(110)$ surface to a little less than 1 ML.

The electronic structure and redox state of the surface at different steps of the fully-hydroxylated $TiO_2(110)$ formation have been examined using UPS with results presented in Fig. 3. It is well-known that the valence band spectrum of clean reduced $TiO_2(110)$ is dominated by O $2p$ emission [26]. On the other hand, the weak Ti $3d$ -derived peak, visible at ~ 0.8 eV in the He I spectrum of the band-gap region in Fig. 3(d) [27], is associated with reduced Ti^{3+} cations related to defect sites [16, 26]. Following the full hydroxylation of the V_O 's via H_2O adsorption in Step I, the OH 3σ feature at ~ 10.4 eV emerges in Fig. 3(c), while the intensity of Ti^{3+} peak in

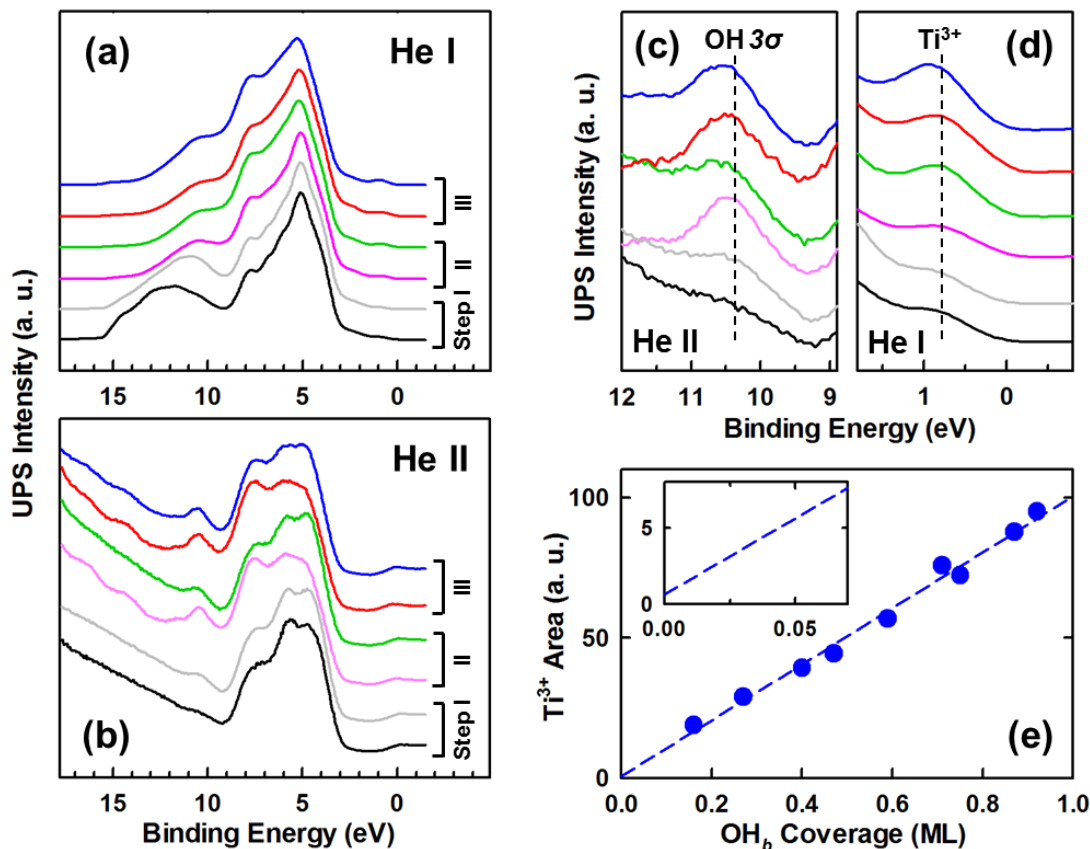


Figure 3. UPS (a) He I and (b) He II spectra, of a clean reduced surface (black) and after: saturation H₂O exposure (grey), first TMAA saturation (pink) and UV irradiation (green), second TMAA saturation (red) and UV irradiation (blue). c) and d) Zoomed-in OH 3 σ and Ti³⁺ regions, respectively. e) Normalized Ti³⁺ peak area as a function of OH_b coverage. The dashed line represents a linear fit. The inset in (e) displays the magnified part near zero OH_b coverage.

Fig. 3(d) remains practically the same, in agreement with previous reports [16, 17]. Upon saturation TMAA exposure in Step II, several features, noticeable in Fig. 3(b) at higher binding energies (~16.3, ~14.2 and ~11.4 eV), are evidently related to TMA species. Moreover, the difference spectrum in Fig. S3 reveals additional TMA-derived peaks at lower binding energies of ~7.8 and ~5.6 eV, as well as one at ~10.2 eV that overlaps with OH 3 σ feature. Concurrently, the OH 3 σ signal notably increases (as clearly seen after subsequent TMA photodepletion), reflecting the addition of extra OH_b species. In contrast, the Ti³⁺ peak in Fig. 3(d) does not grow, indicating that neither hydroxyl formation nor TMA adsorption induce charge transfer/surface reduction, in accord with TMAA dissociation via heterolytic bond cleavage (deprotonation) of

TMAA [23, 24]. After subsequent UV irradiation and a hole-mediated decarboxylation, UPS features of TMA in Fig 3(b) expectedly disappear. On the other hand, a considerable growth of the Ti^{3+} peak is observed, indicating a noticeable increase of the reduction level. This can be attributed to a preferential trapping of the photoexcited electrons, likely, as surface $\text{Ti}^{3+}\text{-OH}_b$ species [23, 28], with Ti trapping sites most likely located in the first subsurface layer [29]. It should be emphasized that the above observations strongly imply that the rise of Ti^{3+} intensity is not caused by an electron transfer from the hydrogen towards the Ti $3d$ levels upon TMAA dissociation and formation of extra OH_b species, but rather by a *photochemical* charging of traps. (It should be also noted that UV irradiation of the clean, OH-free $\text{TiO}_2(110)$ does not result in the increase of Ti^{3+} intensity or any other changes). Finally, as a result of carrying out the last Step III, the UPS spectra once again showed further growth of the OH 3σ peak after additional TMAA dosing, Fig. 3(c), which followed by an additional increase of the Ti^{3+} signal upon UV irradiation (Fig. 3(d)) [30]. Hence, the concluding UPS spectra not only represent the signatures of the fully-hydroxylated $\text{TiO}_2(110)$ surface (such as one represented by STM image in Fig. 2(f), but also reveal rather a high degree of reduction of such surface.

The dependence of the area of defect state peak on the OH_b coverage is shown in Fig. 3(e) (Ti^{3+} integrated intensity was obtained after subtracting secondary electron background, while OH_b coverage was determined from corresponding STM images). It is clear that plot follows a linear fit rather well. While a linear dependence for the Ti^{3+} intensity has been recently reported for relatively low OH_b coverages (< 0.2 ML) [14, 20], our data demonstrate that it is sustained up to saturation coverage of 1 ML. Furthermore, such a direct correlation between the intensity of band-gap defect state and OH_b concentration is consistent with the latter being a trap site for photoexcited electrons [31]. Importantly, the extension of the linear scaling up to a saturation OH_b coverage signifies that the obtained fully-hydroxylated $\text{TiO}_2(110)$ surface is also *fully-reduced* (taking as a reference point the nominal presence of one/two unpaired excess electrons per OH_b/V_O site). A close inspection of the Ti^{3+} area plot in the inset in Fig 3(e) reveals that its extrapolation to zero OH_b coverage intersects rather close to the origin. This supports our prior suggestion [32] in the still ongoing debate [20, 32-34] that other species, unrelated to V_O/OH_b defects, e.g., subsurface Ti interstitials, have rather a minor contribution to the band-gap state in comparison with the surface defects of V_O 's and/or OH_b 's (considering that our method does not introduce any subsurface defects).

We have performed DFT simulations to further verify our conclusions. Figure 4 displays calculated total and selected partial densities of states (DOS) corresponding to experimentally-observed surfaces for each consecutive step. Beyond the valence and conduction bands (derived primarily from O $2p$ and Ti $3d$ states, respectively), the total DOS of the clean reduced $\text{TiO}_2(110)$ surface ($\Theta(V_O) = 0.125$ ML) in Fig. 4(a) also contains the localized Ti $3d$ -derived defect state in the band gap around -1 eV (referenced to the conduction band minimum). In agreement with literature [35], the Ti $3d$ band-gap state is not modified much upon water dissociation at V_O , while an additional peak at ~ -8.7 eV is due to the 3σ states of 0.25 ML of

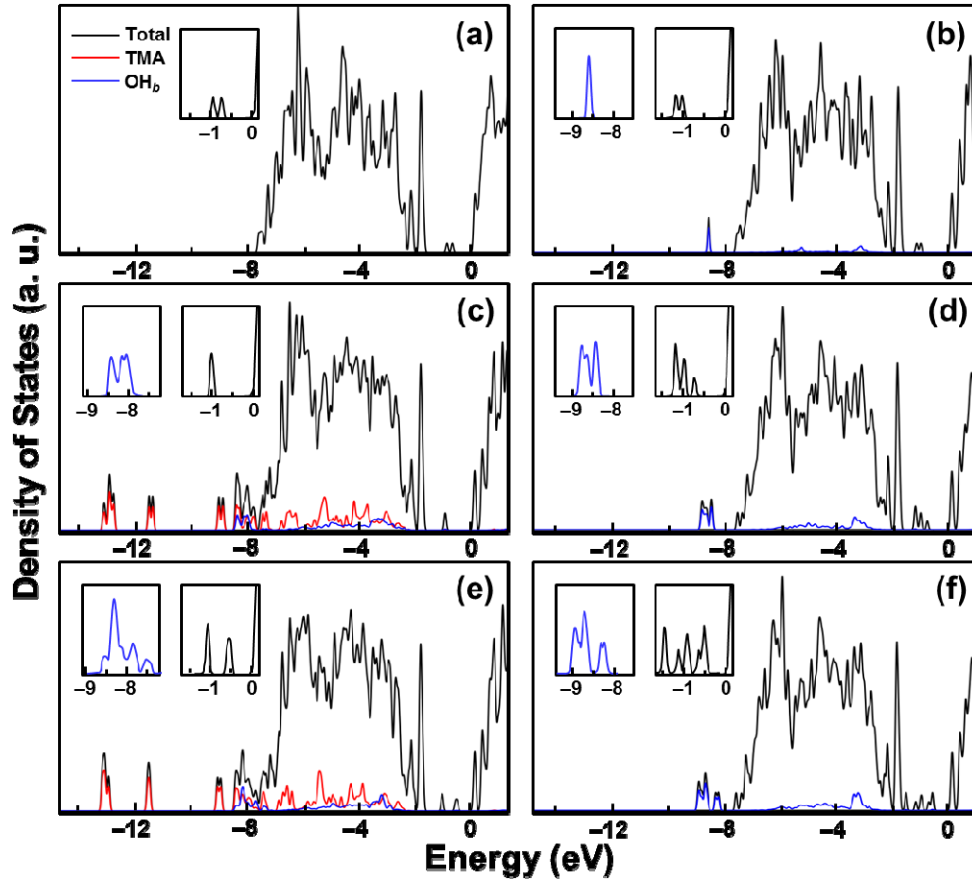


Figure 4. DFT-calculated total and partial DOS of selected $\text{TiO}_2(110)$ surfaces: (a) clean reduced surface, $\Theta(V_O) = 0.125$ ML; (b) $\Theta(\text{OH}_b) = 0.25$ ML; (c) $\Theta(\text{TMA}) = 0.5$ ML, $\Theta(\text{OH}_b) = 0.75$ ML; (d) $\Theta(\text{OH}_b) = 0.75$ ML; (e) $\Theta(\text{TMA}) = 0.5$ ML, $\Theta(\text{OH}_b) = 1$ ML; (f) $\Theta(\text{OH}_b) = 1$ ML OH_b . The insets show zoomed-in OH 3σ and Ti^{3+} states. The zero of energy corresponds to the conduction band minimum.

hydroxyl species, as shown in the insets in Fig. 4(b). The remaining O states of the OH_b 's give a minor contribution to the valence band and are spread within. In a reasonable agreement with UPS spectra in Fig. 3(b), an addition of TMAA (0.5 ML) leads to appearance of several localized/delocalized features in Fig. 4(c) outside/inside the valence band, respectively, which are associated mainly with the methylic carbon and carboxylic oxygen orbitals (see Fig. S6). The concurrent formation of an extra 0.5 ML of OH_b 's upon TMAA deprotonation is reflected in a considerable increase of the OH 3σ area, while, in contrast, the area of Ti $3d$ band-gap states remain nearly the same, as can be seen in the insets in Fig. 4(c). The hydroxylated, TMA-free surface with $\Theta(\text{OH}_b)$ of 0.75 ML and supplemental trapped photoelectrons has been modeled via corresponding addition of atomic hydrogen. These calculations indicate that the density of band-gap states does rise upon the presence of the excess electrons, as shown in Fig. 4(d). Similar trends have been observed for fully-hydroxylated surface ($\Theta(\text{OH}_b) = 1$ ML) with and, ultimately, without TMA, Fig. 4(e) and 4(f), respectively.

There is a clear increase of the number of localized Ti $3d$ states in the band gap for higher OH_b coverages, which correlates well with observed gradual broadening of Ti^{3+} peak in UPS spectra (Fig. S5). Note also that calculated number of excess (Ti^{3+}) electrons is very close to one ($0.99 e$) per OH_b group, though lower fractional charges, e.g., $0.64 e$ [36] and $0.17 e$ [37], have been mentioned in the literature as well. Furthermore, a clear linear correlation between the total excess charge and OH_b coverage can be seen in Fig. S7 (in good agreement with experimental observations in Fig. 3(e)), demonstrating a major contribution of surface defects into the origin of band-gap states. Overall, the DFT-calculated electronic states and experimental UPS analysis agree rather well, providing two independent methods to confirm the reduced nature of the surface at various steps during hydroxylation and support the conclusion that full reduction of 1 ML OH_b 's is possible. Latter underlines the ability of fully-hydroxylated TiO_2 surfaces to stabilize effectively a large amount of excess electrons at trapping (OH) sites without heavy electronic reorganizations. We contemplate that this could be facilitated by an efficient dielectric screening, considering that TiO_2 is a strongly polarizable ($\epsilon_o \sim 100$) oxide. Also note that further studies should explore whether even higher reduction levels could be achieved, e.g., via deposition of electron-donor atoms on the fully-hydroxylated surface.

In conclusion, employing an advanced multi-step photochemical approach, we have prepared a well-ordered, fully-hydroxylated and simultaneously fully-reduced $\text{TiO}_2(110)-(1 \times 1)$ surface,

as demonstrated by STM, UPS and DFT results. These results also exemplify the ability of our method to precisely control OH_b density and thus surface reduction to an arbitrary level up to 1 ML. For surface reactions involving formation of H-containing intermediates, the utmost density of OH groups should allow for increasing concentration of these often elusive species, enabling their detection by conventional spectroscopic techniques (that generally have a rather low sensitivity). Hence, the “super OH” TiO_2 surface may serve as a valuable platform for future mechanistic studies under UHV conditions, related, e.g., to anchoring organometallic complexes or nucleation/growth of metal clusters. Our observations also indicate that hydroxylated TiO_2 surfaces apparently have an inherent mechanism for dealing with a rather large excess of the negative charge, which is critical for sustaining hole-mediated photocatalytic reactions. On the other hand, this extra charge could be potentially transferred to adsorbate species and enable a stronger bonding. Finally, considering that the wetting properties of $\text{TiO}_2(110)$ are mediated largely by the OH groups, the fully-hydroxylated surface may possibly have a “super-hydrophilic” character, which should be verified in the future studies.

We thank M.A. Henderson, G.A. Kimmel, N.G. Petrik, Z. Dohnalek, and Y. Du for stimulating discussions, and also acknowledge computational support from S. Najafi at WPI. This work was supported by the U.S. Department of Energy (DOE), Office of Basic Energy Sciences, Division of Chemical Sciences, and performed at EMSL, a national scientific user facility sponsored by the DOE’s Office of Biological and Environmental Research and located at PNNL.

References

- [1] U. Diebold, Surf. Sci. Rep. **48**, 53 (2003).
- [2] M.A. Henderson, Surf. Sci. Rep. **46**, 1 (2002).
- [3] B.C. Gates, *Catalytic Chemistry* (Wiley, New York, 1992).
- [4] M. Haruta, T. Kobayashi, H. Sano, N. Yamada, Chem. Lett. **16**, 405 (1987).
- [5] Y. Iwasawa (Ed.), *Tailored Metal Catalysts*, Reidel, Dordrecht, 1986.
- [6] N.G. Petrik, G.A. Kimmel, J. Phys. Chem. Lett. **1**, 2508 (2010).
- [7] Y. Du, N.A. Deskins, Z. Zhang, Z. Dohnalek, M. Dupuis, I. Lyubinetsky, Phys. Rev. Lett. **102**, 096102 (2009).
- [8] R. Wang, N. Sakai, A. Fujishima, T. Watanabe, K. Hashimoto, J. Phys. Chem. B **103**, 2188 (1999).
- [9] G. Ketteler, S. Yamamoto, H. Bluhm, K. Andersson, D.E. Starr, D.F. Ogletree, H. Ogasawara, A. Nilsson, M. Salmeron, J. Phys. Chem. C **111**, 8278 (2007).
- [10] Z. Dohnalek, I. Lyubinetsky, R. Rousseau, Prog. Surf. Sci. **85**, 161 (2010).
- [11] M.A. Henderson, I. Lyubinetsky, Chem. Rev. **113**, 4428 (2013).
- [12] N.G. Petrik, G.A. Kimmel, J. Phys. Chem. C **113**, 4451 (2009).
- [13] S. Suzuki, K.-i. Fukui, H. Onishi, Y. Iwasawa, Phys. Rev. Lett. **84**, 2156 (2000).
- [14] X.L. Yin, M. Calatayud, H. Qiu, Y. Wang, A. Birkner, C. Minot, C. Wöll, ChemPhysChem **9**, 253 (2008).
- [15] Y. Yoon, Y. Du, J.C. Garcia, Z. Zhu, Z.-T. Wang, N.G. Petrik, G.A. Kimmel, Z. Dohnalek, M.A. Henderson, R. Rousseau, N.A. Deskins, I. Lyubinetsky, ChemPhysChem **16**, 313 (2015).
- [16] R.L. Kurtz, R. Stockbauer, T.E. Madey, E. Roman, J.L.d. Segovia, Surf. Sci. **218**, 178 (1989).
- [17] V.E. Henrich, G. Dresselhaus, H.J. Zeiger, Solid State Commun. **24**, 623 (1977).
- [18] P.M. Kowalski, B. Meyer, D. Marx, Phys. Rev. B **79**, 115410 (2009).
- [19] Y. Du, N.G. Petrik, N.A. Deskins, Z. Wang, M.A. Henderson, G.A. Kimmel, I. Lyubinetsky, Phys. Chem. Chem. Phys. **14**, 3066 (2012).
- [20] X. Mao, X. Lang, Z. Wang, Q. Hao, B. Wen, Z. Ren, D. Dai, C. Zhou, L.-M. Liu, X. Yang, J. Phys. Chem. Lett., 3839 (2013).
- [21] Z.-T. Wang, N.A. Deskins, M.A. Henderson, I. Lyubinetsky, Phys. Rev. Lett. **109**, 266103 (2012).
- [22] See Supplemental Material, which includes Refs. [38-42], at <http://links.aps.org/> for experimental and computational details.
- [23] M.A. Henderson, J.M. White, H. Uetsuka, H. Onishi, J. Am. Chem. Soc. **125**, 14974 (2003).
- [24] I. Lyubinetsky, Z.Q. Yu, M.A. Henderson, J. Phys. Chem. C **111**, 4342 (2007).
- [25] I. Lyubinetsky, N.A. Deskins, Y. Du, E.K. Vestergaard, D.J. Kim, M. Dupuis, Phys. Chem. Chem. Phys. **12**, 5986 (2010).
- [26] Z. Zhang, S.-P. Jeng, V.E. Henrich, Phys. Rev. B **43**, 12004 (1991).

- [27] It is rather hard to discern the Ti^{3+} peak in He II spectrum due to its overlapping with a stronger satellite feature generated by unmonochromated He II radiation (Fig. 3(b)).
- [28] S.H. Szczepankiewicz, A.J. Colussi, M.R. Hoffmann, *J. Phys. Chem. B* **104**, 9842 (2000).
- [29] N.A. Deskins, R. Rousseau, M. Dupuis, *J. Phys. Chem. C* **113**, 14583 (2009).
- [30] The apparent shift of OH 3σ and Ti^{3+} peaks toward higher binding energy in Fig. 3(c) and 3(d) is due to band-bending that gradually increases upon further hydroxylation and reduction (Fig. S4).
- [31] The width of the Ti^{3+} peak also proportionally increases with OH_b coverage (Fig. S5), which is consistent with a growing electron population of the band-gap defect state upon further reduction.
- [32] Y. Du, N.A. Deskins, Z. Zhang, Z. Dohnalek, M. Dupuis, I. Lyubinetsky, *Phys. Chem. Chem. Phys.* **12**, 6337 (2010).
- [33] S. Wendt, P.T. Sprunger, E. Lira, G.K.H. Madsen, Z. Li, J.O. Hansen, J. Matthiesen, A. Blekinge-Rasmussen, E. Laegsgaard, B. Hammer, F. Besenbacher, *Science* **320**, 1755 (2008).
- [34] C.M. Yim, C.L. Pang, G. Thornton, *Phys. Rev. Lett.* **104**, 036806 (2010).
- [35] C. Di Valentin, G. Pacchioni, A. Selloni, *Phys. Rev. Lett.* **97**, 166803 (2006).
- [36] S.-C. Li, Z. Zhang, D. Sheppard, B.D. Kay, J.M. White, Y. Du, I. Lyubinetsky, G. Henkelman, Z. Dohnalek, *J. Am. Chem. Soc.* **130**, 9080 (2008).
- [37] Z. Li, D.V. Potapenko, R.M. Osgood, *ACS Nano* **9**, 82 (2015).
- [38] Z.Q. Yu, C.M. Wang, Y. Du, S. Thevuthasan, I. Lyubinetsky, *Ultramicroscopy* **108**, 873 (2008).
- [39] G. Kresse, J. Hafner, *Phys. Rev. B* **47**, 558 (1993).
- [40] G. Kresse, D. Joubert, *Phys. Rev. B* **59**, 1758 (1999).
- [41] J.P. Perdew, K. Burke, M. Ernzerhof, *Phys. Rev. Lett.* **77**, 3865 (1996).
- [42] S.L. Dudarev, G.A. Botton, S.Y. Savrasov, C.J. Humphreys, A.P. Sutton, *Phys. Rev. B* **57**, 1505 (1998).